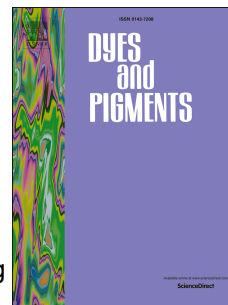


# Journal Pre-proof

A “turn-on” near-infrared fluorescent probe with high sensitivity for detecting reduced glutathione based on red shift *in vitro* and *in vivo*

Kaiping Wang, Gang Nie, Siqi Ran, Huiling Wang, Xiqiu Liu, Ziming Zheng, Yu Zhang



PII: S0143-7208(19)31643-2

DOI: <https://doi.org/10.1016/j.dyepig.2019.107837>

Reference: DYPI 107837

To appear in: *Dyes and Pigments*

Received Date: 16 July 2019

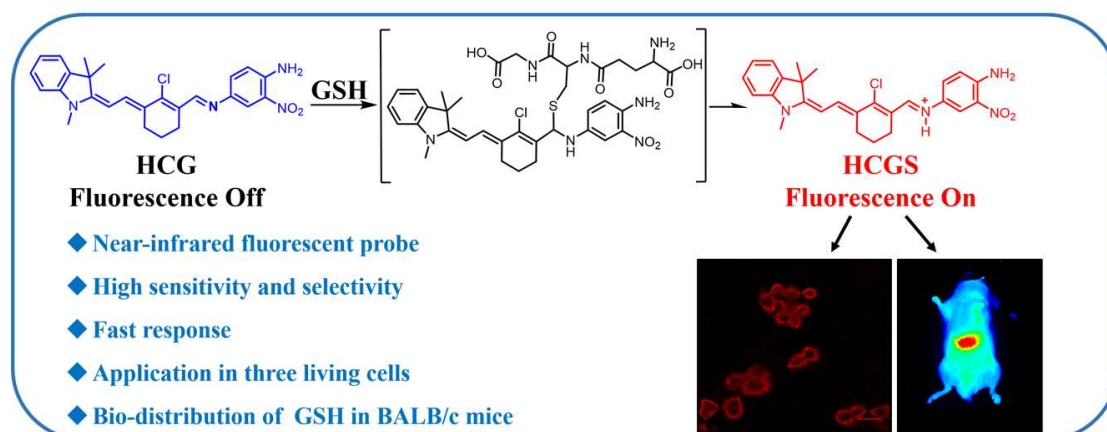
Revised Date: 24 August 2019

Accepted Date: 24 August 2019

Please cite this article as: Wang K, Nie G, Ran S, Wang H, Liu X, Zheng Z, Zhang Y, A “turn-on” near-infrared fluorescent probe with high sensitivity for detecting reduced glutathione based on red shift *in vitro* and *in vivo*, *Dyes and Pigments* (2019), doi: <https://doi.org/10.1016/j.dyepig.2019.107837>.

This is a PDF file of an article that has undergone enhancements after acceptance, such as the addition of a cover page and metadata, and formatting for readability, but it is not yet the definitive version of record. This version will undergo additional copyediting, typesetting and review before it is published in its final form, but we are providing this version to give early visibility of the article. Please note that, during the production process, errors may be discovered which could affect the content, and all legal disclaimers that apply to the journal pertain.

© 2019 Published by Elsevier Ltd.



In this manuscript, a “turn-on” near-infrared fluorescent probe was developed and applied to monitor glutathione (GSH) with excellent sensitivity and selectivity *in vitro*. The novel probe HCG was successfully applied to detect endogenous and exogenous GSH in three living cells and the bio-distribution of GSH in BALB/c mice.

1     **A “turn-on” near-infrared fluorescent probe with high sensitivity for detecting**  
2                   **reduced glutathione based on red shift *in vitro* and *in vivo*.**

3     Kaiping Wang<sup>a</sup>, Gang Nie<sup>a</sup>, Siqi Ran<sup>a</sup>, Huiling Wang<sup>c</sup>, Xiqiu Liu<sup>a</sup>, Ziming Zheng<sup>b</sup> and  
4                   Yu Zhang<sup>b,\*</sup>

5     <sup>a</sup>Hubei Key Laboratory of Nature Medicinal Chemistry and Resource Evaluation,  
6     Tongji Medical College of Pharmacy, Huazhong University of Science and  
7     Technology, Wuhan, China

8     <sup>b</sup>Union Hospital of Tongji Medical College, Huazhong University of Science and  
9     Technology, Wuhan, China

10    <sup>c</sup>Key Laboratory of Pesticide and Chemical Biology, Ministry of Education, Chemical  
11    Biology Center, College of Chemistry, and International Joint Research Center for  
12    Intelligent Biosensing Technology and Health, Central China Normal University,  
13    Wuhan, China

14    \*Corresponding author: Dr. and Prof. Yu Zhang, Email: zhangwkp@163.com

15    **Abstract**

16        Fluorescence imaging has become a powerful tool for detecting reduced  
17    glutathione (GSH) to comprehend the physiological and pathological roles of GSH  
18    and the potential clinical diagnosis of GSH-related diseases, such as AIDS, liver  
19    damage, cancer, and leucocyte loss. High sensitivity and high selectivity remain  
20    challenges for near-infrared fluorescent probes to monitor GSH. Herein, a turn-on  
21    near-infrared fluorescent probe (HCG) was designed and developed in a convenient  
22    synthetic procedure, which had high sensitivity and selectivity to detect GSH based on

23 the red shift of Schiff base. HCG could discriminate against amino acid that resemble  
24 GSH to monitor GSH *in vitro*. The fluorescence emission intensity linearly increased  
25 with an increasing concentration of GSH in the range of 0-16  $\mu\text{M}$ , with a limit  
26 detection of 252 nM. HCG exhibited a diminutive detection limit (0.5  $\mu\text{M}$  in actual  
27 experiments), a fast response time (30 s) and low cytotoxicity. The detection  
28 mechanism was confirmed by HPLC and HRMS spectra. Furthermore, HCG  
29 exhibited an excellent capacity for fluorescence imaging and has been successfully  
30 applied to detect endogenous GSH in three living cells. Finally, the bio-distribution of  
31 GSH in BALB/c mice was studied by using HCG. The results suggest that HCG has  
32 potential utility in biological science research.

33 **Keywords:** *Near-infrared fluorescent probe; Reduced glutathione detection; High*  
34 *sensitivity and selectivity; Schiff base's red shift; Fluorescence imaging; Facile*  
35 *synthetic procedures.*

## 36 1. Introduction

37 Intracellular biothiols, including reduced glutathione (GSH), cysteine (Cys), and  
38 homocysteine (Hcy), act as significant roles in many biological processes [1-3]. It is  
39 deserved to be mentioned that GSH is widely distributed in living organisms and can  
40 serve as a biomarker in the biological system among intracellular bio-thiols [4]. As  
41 reported in literatures [5-8], GSH can contribute to an improvement in immunity and  
42 anti-aging among physiological processes and GSH is a great scavenger for reactive  
43 oxygen to maintain the appropriate physiological redox state . However, aberrant GSH  
44 levels have been associated with a variety of diseases, such as AIDS, liver damage,

45 cancer, and leucocyte loss [9-11]. Based on these disease features, traditional  
46 analytical method has been developed for detecting GSH by high-performance liquid  
47 chromatography and mass spectrometry [5]. However, it is difficult to prepare  
48 biological samples and monitor GSH in real time. Thus, many new strategies have  
49 been gradually used to monitor GSH in biological models [12-15]. Among these  
50 strategies, fluorescence imaging has been paid great attention for the detection of  
51 GSH in biological systems [16-18]. Different kinds of fluorescent probes have been  
52 developed for detecting GSH on the basis of different reaction mechanisms, such as  
53 Michael addition [19, 20], nucleophilic substitution [21], cyclization with an aldehyde  
54 [22], Se-N cleavage by thiols [23], the elimination of disulfide [24] and others [25-27].  
55 In the reported fluorescent probes for the detection of GSH, there are strong  
56 interference from Cys and Hcy, due to their similar molecular structures and  
57 nucleophilicity. So, it is still a challenge to develop a highly specific fluorescent probe  
58 for detecting GSH. [28-31].

59 In recent years, near-infrared fluorescent probes have increasingly been applied  
60 to detect GSH, due to the reduced biological damage and deeper tissue penetration of  
61 the light in this wavelength region [21, 28, 31-34]. Near-infrared fluorescent probes  
62 contain low photon absorption and can provide high-resolution fluorescence intensity  
63 to produce effective fluorescent signals *in vitro* and *in vivo* without fluorescent  
64 interference. Compared with non-near-infrared fluorescent probes, near-infrared  
65 fluorescent probes have greater sensitivity and more extensive applications [35].  
66 Taking advantage of these near-infrared fluorescent probes, several turn-on and

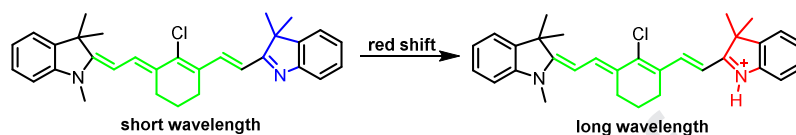
67 ratiometric near-infrared fluorescent probes have been developed for detecting GSH  
68 [32-34]. The detection moieties of these near-infrared fluorescent probes still utilize  
69 the nucleophilicity of GSH to lead to low selectivity for discriminating against amino  
70 acids that resemble GSH. Moreover, these probes exhibited slow response time and  
71 their synthetic routes were complicated. Based on the shortcomings of the existing  
72 fluorescent probes, it is still of great importance to develop a more sensitive and  
73 selective near-infrared probe to detect intracellular GSH through a convenient  
74 synthetic procedure.

75 As reported in the literature [36-41], non-N-alkylated cyanine dyes include a  
76 protonatable amino group with an indole group. When the indole nitrogen atom  
77 deprotonates, it absorbs in the short wavelength region. The dye will have a strong red  
78 fluorescence when the indole nitrogen atom has a proton. This change occurs over a  
79 very short time, which means that a more sensitive probe with an indole nitrogen atom  
80 moiety may be designed to detect GSH, and suggests an excellent spectroscopic  
81 window to monitor the turning off or on of a visual optical signal (Scheme 1). This  
82 strategy offers a new way to design near-infrared fluorescent probes. Encouraged by  
83 this mechanism, we hope to develop a highly sensitive and selective near-infrared  
84 fluorescent probe with a similar structure to detect GSH.

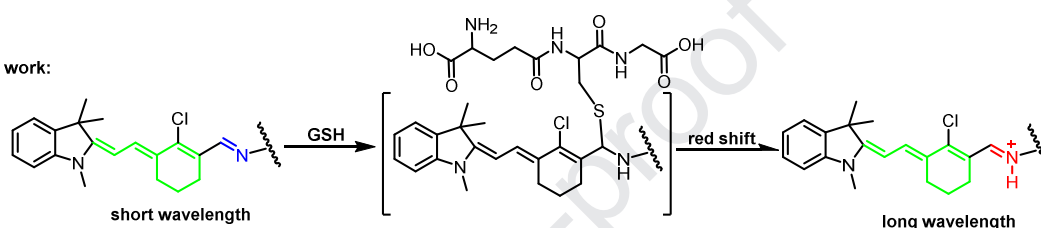
85 Herein, making use of this shift strategy, we report the turn-on hemi-cyanine  
86 fluorescent probe HCG with excellent sensitivity and selectivity based on a Schiff  
87 base redshift reaction for the detection of GSH *in vitro*. Moreover, HCG was  
88 successfully applied to three living cells and the BALB/c mice to detect GSH by

89 fluorescence imaging. The fluorescent images showed that using HCG to detect GSH  
 90 is helpful to understand the possible biogenesis approaches of endogenous GSH *in*  
 91 *vivo*. The results indicated that HCG was an effective tool for monitoring GSH in  
 92 bioscience research.

1. Non-N-alkylated cyanine dyes:



2. This work:



93

94

95

**Scheme 1. Schiff base redshift**

## 96 2. Experimental

### 97 2.1 Reagents and apparatus

98 All commercial chemicals were of analytical reagent grade and used without  
 99 further purification. All reactions were monitored by TLC and the TLC plate was  
 100 detected by ultraviolet light (254 nm or 365 nm). Silica gel column chromatography  
 101 was used to purify the compound. A reduced glutathione (GSH) assay kit was  
 102 obtained from Jiancheng Bioengineering Institute (Nanjing, China).  $^1\text{H-NMR}$  and  
 103  $^{13}\text{C-NMR}$  spectra were acquired on a Bruker NMR 400MHz spectrometer. The high  
 104 resolution mass spectra of all compounds were recorded by FT-MS (Bruker Daltonics  
 105 SolariX 7.0T). The UV spectra were obtained with UV/VIS (Jena , Specord 210)  
 106 spectrophotometer in 1 cm quartz cells. Fluorescence excitation and emission spectra

107 were measured on a Hitachi F-4600 fluorescence spectrophotometer. Fluorescent  
108 images of cells were obtained with a confocal laser scanning microscope (Nikon A1).  
109 Fluorescent images of BALB/c were recorded by a small-animal *in vivo* imaging  
110 system (IVIS).

## 111 2.2 Synthesis of HCG

112 The synthesis procedures of the other compounds are shown in Scheme S1. Cy7  
113 (300 mg, 1.037 mmol) and 2-nitrobenzene-1,4-diamine (190 mg, 1.244 mmol) were  
114 dissolved in 5 mL of anhydrous DMSO. Then, N,N-diisopropylethylamine (100  $\mu$ L)  
115 was added to the reaction mixture. The reaction was kept at 60 °C for 24 h under  
116 nitrogen atmosphere. Next, the solvent was removed under reduced pressure to obtain  
117 the crude product, which was purified by column chromatography on silica gel with a  
118 gradient of ethyl acetate ; petroleum ether from 10:1 to 3:1 (v/v), and the black solid  
119 HCG was finally obtained (153.3 mg, 32%). <sup>1</sup>H-NMR (400 MHz, CDCl<sub>3</sub>)  $\delta$  8.91 (s,  
120 1H), 8.02 (d, J = 2.4 Hz, 1H), 7.65 (d, J = 12.7 Hz, 1H), 7.41 (dd, J = 8.8, 2.4 Hz, 1H),  
121 7.26 – 7.18 (m, 2H), 6.95 – 6.83 (m, 2H), 6.70 (d, J = 7.8 Hz, 1H), 6.13 (s, 2H), 5.47  
122 (d, J = 12.7 Hz, 1H), 3.22 (s, 3H), 2.77 (t, J = 6.1 Hz, 2H), 2.67 – 2.60 (m, 2H), 1.91 –  
123 1.83 (m, 2H), 1.69 (s, 6H). <sup>13</sup>C-NMR (100 MHz, CDCl<sub>3</sub>)  $\delta$  160.8 (s), 158.5 (s), 144.8  
124 (s), 142.8 (s), 142.8 (s), 141.9 (s), 139.1 (s), 132.2 (s), 130.8 (s), 128.9 (s), 127.8 (s),  
125 124.5 (s), 121.7 (s), 120.3 (s), 119.3 (s), 117.1 (s), 106.3 (s), 92.9 (s), 46.1 (s), 29.3 (s),  
126 28.3 (s), 26.7 (s), 26.6 (s), 21.4 (s). HRMS (ESI<sup>+</sup>): m/z found [M+H]<sup>+</sup> 463.1889.  
127 molecular formula C<sub>26</sub>H<sub>28</sub>ClN<sub>4</sub>O<sub>2</sub><sup>+</sup>, requires [M+H]<sup>+</sup> 463.1895.

## 128 2.3 Cell culture and fluorescent imaging

129 MCF-7, HT-29 and HepG2 cells were incubated in DMEM supplemented with  
130 10 % (v/v) FBS, penicillin (100 U/mL) and streptomycin (100 µg/mL) at 37°C under  
131 a humidified atmosphere containing 5 % CO<sub>2</sub>. For fluorescence imaging, cells were  
132 pretreated with varying concentrations of GSH or other analytes in 12-well plates (1×  
133 10<sup>6</sup> cells/well) at 37°C for the appropriate time. Then, the cells were washed with  
134 HEPES (10 mM, pH=7.4) and incubated with a mixture of fresh DMEM and an  
135 administered the probe HCG (10 µM) at 37 °C for 15 min. Fluorescence images were  
136 acquired with a confocal laser scanning microscope. The fluorescence detection  
137 setting were kept constant throughout all imaging experiments.

#### 138 2.4 General flow cytometry methods

139 In general, for flow cytometry, the cells were incubated with different  
140 concentrations of GSH, and GSH scavengers in 12-well plates (1× 10<sup>6</sup> cells/well) at  
141 37°C for a certain amount of time. Then, the cells were washed with HEPES (10 mM,  
142 pH=7.4) and incubated with a mixture of fresh DMEM without fetal bovine serum  
143 and administered HCG (10 µM) at 37° C for 15 min. Subsequently, the cells with  
144 HEPES were analyzed by flow cytometry (BD, Accuri™ C6) equipped with 640 nm  
145 excitation laser light line source.

#### 146 2.5 Fluorescence imaging in BALB/c mice

147 BALB/c mice were divided into two groups. The control group mice were  
148 pre-injected with saline for 5 min and GSH group mice were pre-injected with  
149 concentration of GSH (1 mM) for 5 min. Next, all mice were injected with HCG (10  
150 µM, 100 µL in 1:99 DMSO/saline, v/v). The probe was incubated in BALB/c mice for

151 30 min and the fluorescent images of the BALB/c mice were obtained by a  
152 small-animal *in vivo* imaging system (IVIS).

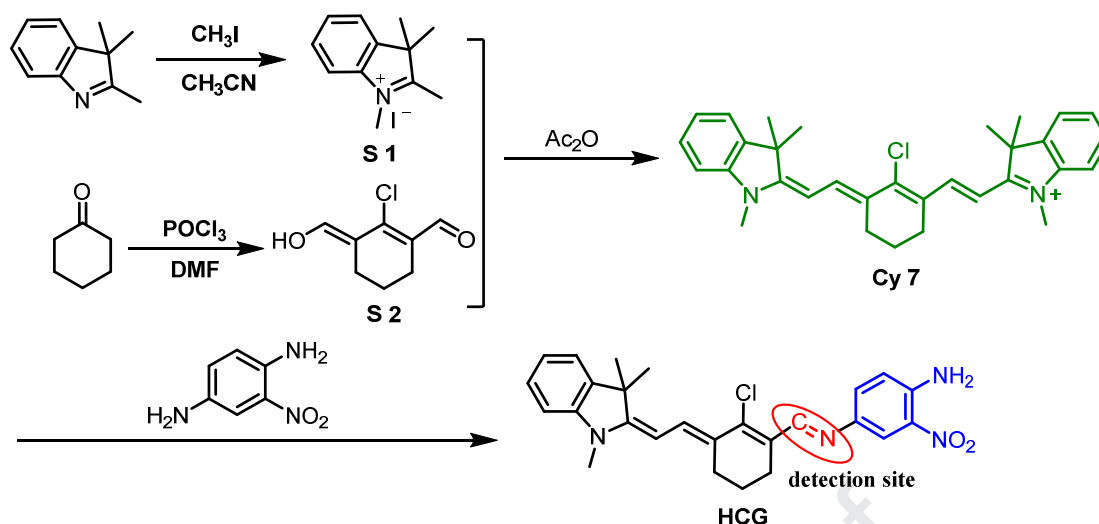
### 153 2.6 High-performance liquid chromatography (HPLC) analysis

154 The HPLC technique was employed in the reaction mechanism experiment.  
155 HPLC was used to monitor the process by which the probe HCG (10  $\mu$ M) reacted  
156 with 500  $\mu$ M GSH for 15 min. The retention time of each compound was confirmed  
157 so that a better understanding of the reaction mechanism could be obtained.

## 158 3. Results and discussion

### 159 3.1 Design and synthesis of probe HCG

160 Because protonatable amino groups can undergo a red shift, we hoped to design  
161 a similar structure. The Schiff base also contains a protonatable nitrogen atom and can  
162 produce a red emission optical signal. Meanwhile, the Schiff base moiety can be  
163 synthesized conveniently. Thus, for the purpose of constructing a turn on fluorescent  
164 probe, 1,2,3,3-tetramethyl-3H-indole and  
165 (E)-2-chloro-cyclohex-1-ene-1-carbaldehyde were synthesized by known conditions  
166 initially. Next, compound **S1** reacted with compound **S2** under aldol condensation  
167 conditions to give Cyanine 7. The probe HCG was obtained in one step by the  
168 combination compound Cy7 and 2-nitrobenzene-1,4-diamine [42, 43]. HCG contains  
169 a Schiff base structure, which is the core of the probe and can serve as the recognition  
170 group for GSH. Moreover, the withdrawing group of probe HCG is beneficial to  
171 produce a large red shift emission in the fluorescence spectrum signal. Compared with  
172 traditional synthetic approaches, this procedure was more convenient. (Scheme 2).



173

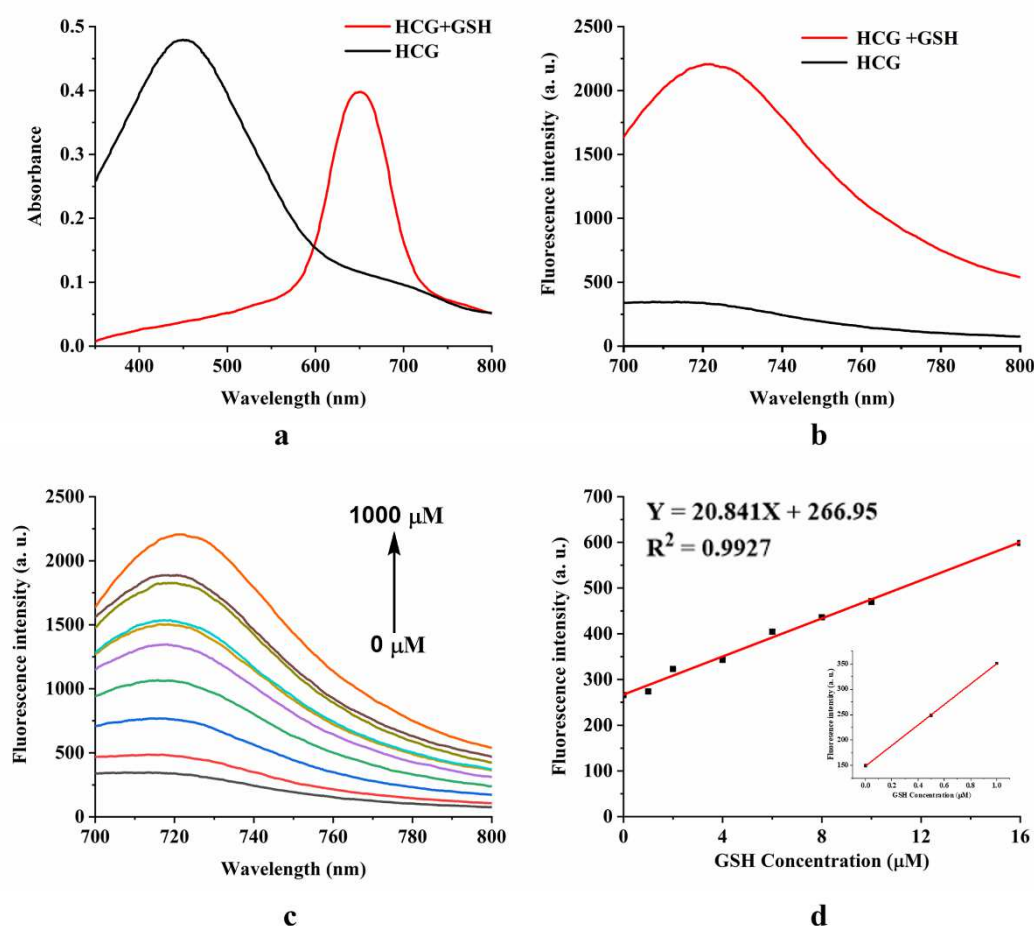
174

Scheme 2. The synthetic procedure of probe HCG

## 175 3.2 Spectroscopic properties and sensitivity of the probe HCG

176 Our studies began by examining the UV/Vis absorption and fluorescence spectra  
 177 of HCG and  $10\ \mu\text{M}$  HCG reacted with  $500\ \mu\text{M}$  GSH. The results indicated that the  
 178 maximum absorption wavelength of HCG was located at 450 nm. Interestingly, after  
 179 reacting with GSH, its maximum absorption wavelength was observed in the 653 nm  
 180 region (Fig 1a). In the fluorescence spectra, there is a weak fluorescence emission  
 181 from HCG at 720 nm. After  $500\ \mu\text{M}$  GSH was added followed by incubation for 1  
 182 min, the fluorescence intensity increased 8-fold at 720 nm (Fig 1b). This result  
 183 indicated that HCG is a turn on near-infrared fluorescent probe and has a short  
 184 detection time. The fluorescent quantum yield of HCG reacted with GSH was 17%  
 185 relative to Oxazine 1 ( $\Phi_{\text{oxz}}=0.14$  in EtOH) [44]. To test the sensitivity of HCG, the  
 186 fluorescence spectra of HCG ( $10\ \mu\text{M}$ ) reacted with varying concentrations of GSH  
 187 (0-1000  $\mu\text{M}$ ) were recorded by fluorescence spectrophotometry. The results showed  
 188 that the fluorescence intensity increased and reached a gradual plateau with increasing  
 189 concentration of GSH (Fig 1c and S1c). Moreover, it was found that the fluorescence

190 emission intensity linearly increased with the concentration of GSH in the range of  
 191 0-16  $\mu\text{M}$  and the detection limit (DL) of HCG was calculated to be 252 nM  
 192 (signal-to-noise ratio (S/N) = 3). In the real detection experiment, the DL of HCG was  
 193 0.5  $\mu\text{M}$  (Fig 1d). There is a reduced glutathione (GSH) assay kit from Jiancheng  
 194 Bioengineering Institute (Nanjing, China), whose DL is 451 nM and the real detection  
 195 limit is 1.5  $\mu\text{M}$  (Fig S1). Compared with this commercial kit, HCG has higher  
 196 sensitivity.

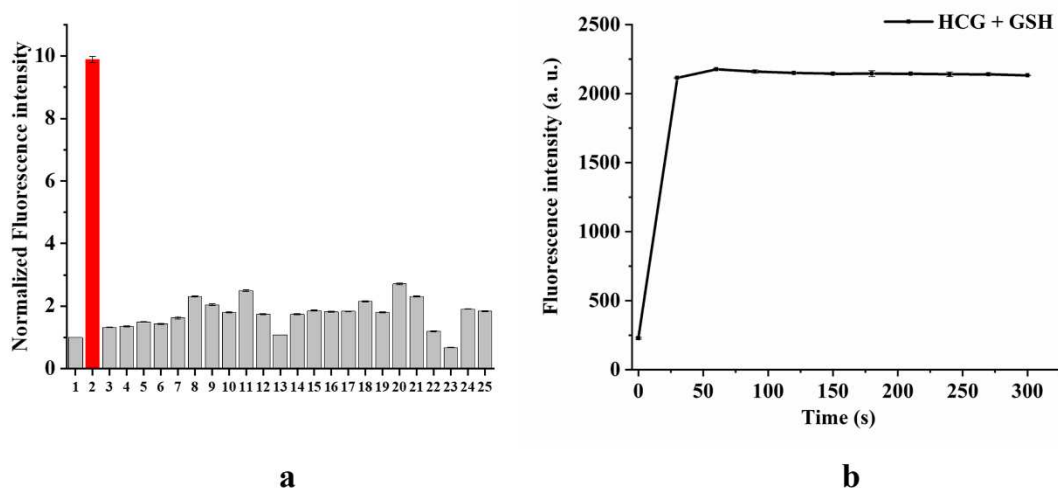


197  
 198 **Fig 1. The UV spectra and fluorescence emission spectra of HCG in response to GSH.** a)  
 199 Black: Absorbance spectrum of HCG (10  $\mu\text{M}$ ) in DMSO/HEPES buffer (10 mM, 1:10, v/v, pH 7.4)  
 200 at 25  $^{\circ}\text{C}$ , Red: Absorbance spectrum of 10  $\mu\text{M}$  HCG reacted with 500  $\mu\text{M}$  GSH in DMSO/HEPES  
 201 buffer (10 mM, 1:10, v/v, pH 7.4) at 25  $^{\circ}\text{C}$  for 15 min; b) Fluorescence emission spectra of HCG,

202 and 10  $\mu\text{M}$  HCG with 500  $\mu\text{M}$  GSH in DMSO/HEPES buffer (10 mM, 1:10, v/v, pH 7.4) at  
203 37  $^{\circ}\text{C}$  for 1 min; c) Fluorescence emission spectra of HCG (10  $\mu\text{M}$ ) with various concentrations of  
204 GSH (0, 10, 20, 40, 60, 80, 100, 200, 500, 1000  $\mu\text{M}$ ) at 37  $^{\circ}\text{C}$  for 15 min; d) Linear correlation of  
205 fluorescence emission intensity towards GSH concentration and the real experimental detection  
206 limit. ( $\lambda_{\text{ex}} = 653 \text{ nm}$ ).

### 207 3.3 Selectivity of the probe HCG

208 To examine the selectivity of HCG, different amino acids and other species were  
209 introduced to HCG, such as Cys, GSH, Ala, Pro, Lys, Thr, His, Val, Tyr, Ser, Phe, Arg,  
210 Trp, Met, Leu, Asp, Gly, Ile, Gln, Hcy and others. As shown in Fig 2a, only GSH can  
211 be monitored by HCG among all the amino acids tested. It is worth mentioning that  
212 the fluorescence intensity of the reaction of HCG with Cys, Hcy and GSH showed a  
213 large difference, indicating that there is good anti-interference and high selectivity for  
214 HCG to react with GSH compared with similar amino acids. In addition, the  
215 time-dependence was measured to explore the time required for HCG to respond to  
216 GSH. Excitingly, when GSH was added into the HCG buffer solution, the  
217 fluorescence intensity increased immediately and achieved a balance within 30 s (Fig  
218 2b), suggesting that HCG has a great response to GSH and exhibits excellent  
219 sensitivity. A possible interpretation is that the Schiff base redshift emission leads to a  
220 rapid response to GSH.



221

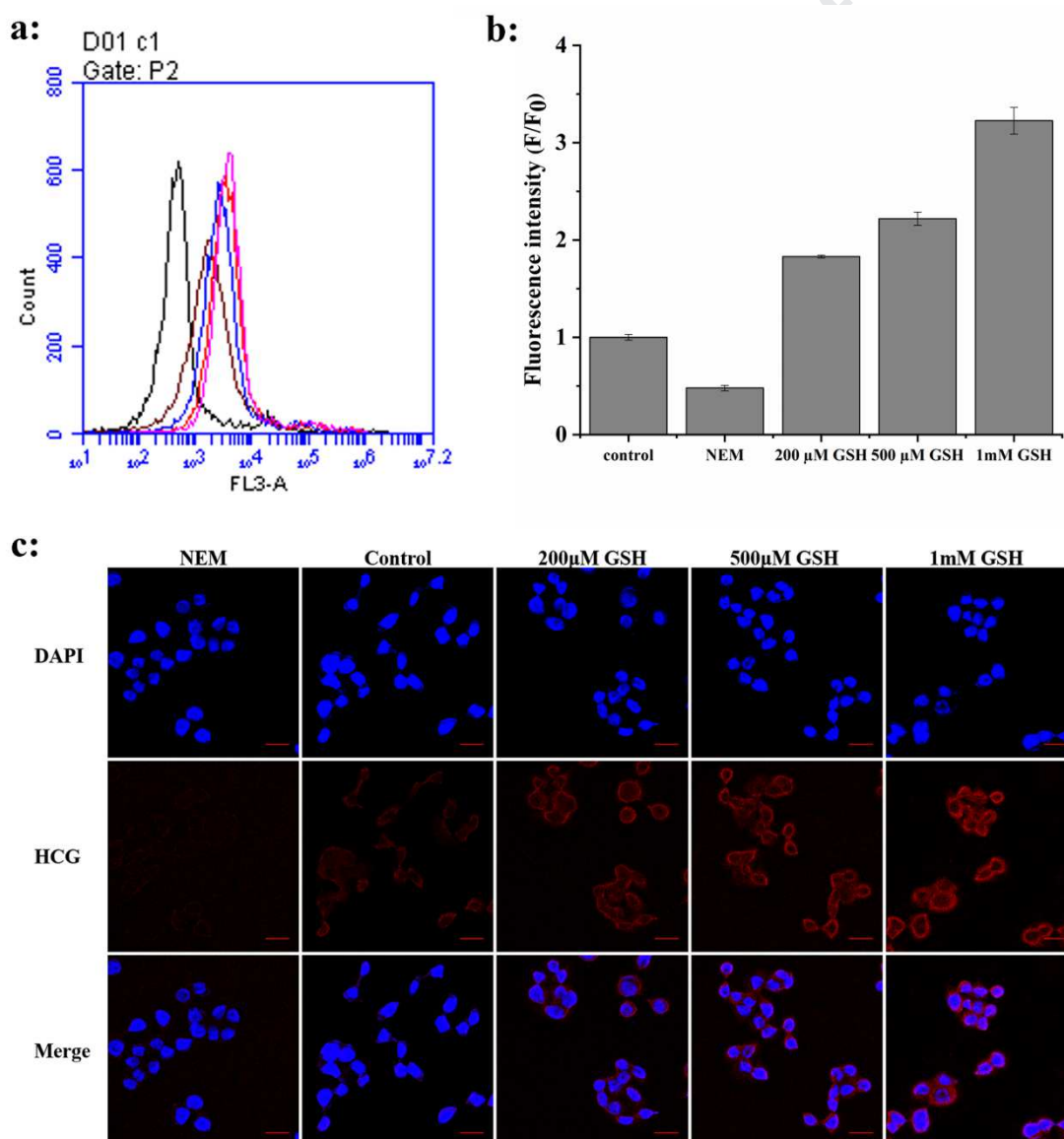
222 **Fig 2. The selectivity and kinetics of the HCG response to GSH.** a) Fluorescence responses of  
 223 10  $\mu\text{M}$  HCG to 500  $\mu\text{M}$  of biologically relevant species in DMSO/HEPES buffer (10 mM, 1:10,  
 224 v/v, pH 7.4) at 37  $^{\circ}\text{C}$  for 15 min: (1) probe, (2) GSH, (3) Cys, (4) Ala, (5) Pro, (6) Lys, (7) Thr, (8)  
 225 His, (9) Val, (10) Tyr, (11) Ser, (12) Phe, (13) Arg, (14) Cystine, (15) Trp, (16) Met, (17) Leu, (18)  
 226 Asp, (19) Gly, (20) Ile, (21) Gln, (22)  $\text{HSO}_3^-$ , (23)  $\text{SO}_3^{2-}$ , (24)  $\text{H}_2\text{O}_2$ , (25) Hcy; b) Kinetics of 500  
 227  $\mu\text{M}$  GSH detected by 10  $\mu\text{M}$  HCG at 37 $^{\circ}\text{C}$  in HEPES (pH 7.4) ( $\lambda_{\text{ex}} = 653 \text{ nm}$ ).

228 3.4 Flow cytometry analysis of GSH and confocal microscopy images in living cells  
 229 using HCG

230 Based on the good fluorescent properties of HCG in buffer, HCG was applied to  
 231 detect GSH in living cells. The cytotoxicity of HCG was established firstly, using  
 232 MTT assays with MCF-7, HT-29 and HepG2 cells. The cell viabilities exceeded 92%  
 233 when incubated with 10  $\mu\text{M}$  HCG. In the range of 0-100  $\mu\text{M}$  HCG, the cell viabilities  
 234 were still over 82%, demonstrating the low cytotoxicity of the probe HCG in living  
 235 cells (Fig S2). Furthermore, the fluorescence intensity of HCG was weak and stable in  
 236 the range of pH 5-10. When added GSH into the solution of HCG, the fluorescence  
 237 intensity of HCG response to GSH had a significant improvement in the range of pH

238 5-10 (Fig S3). As shown in Fig S2 and S3, the results above demonstrated that HCG  
239 was stable and suitable for cell imaging under biological conditions. On the basis of  
240 these results, flow cytometry was used to analyze of the fluorescence intensity of  
241 HCG in response to GSH in MCF-7, HT-29 and HepG2 cells. HT-29 cells were  
242 pretreated with different concentrations of GSH (0, 200, 500, 1000  $\mu$ M) for 30 min,  
243 followed by, incubation with 10  $\mu$ M HCG for 15 min and analysis by flow cytometry.  
244 As shown in Fig 3a, the fluorescence intensity of the HCG response to GSH improved  
245 with increasing GSH concentration. N-ethylmaleimide (NEM, 2 mM), a well-known  
246 scavenger of biothiols [45, 46], was pretreated with HT-29 cells for 30 min, and then  
247 subsequently, incubated with 10  $\mu$ M HCG for 15 min and analyzed by flow cytometry.  
248 The flow cytometry data showed that the fluorescence intensity of HT-29 cells  
249 incubated with NEM decreased to half that of the control group (Fig 3b). The flow  
250 cytometry results in MCF-7 cells and HepG2 cells were analogous to those in HT-29  
251 cells (Fig S4). Encouraged by the results above, confocal microscopy imaging was  
252 applied to HT-29, MCF-7 and HepG2 cells. HT-29 cells were incubated with different  
253 concentrations of GSH (0, 200, 500, 1000  $\mu$ M) for 30 min. Next, the cells were  
254 treated with 10  $\mu$ M HCG for additional 15 min, and fluorescent images were acquired  
255 by confocal microscopy. As shown in Fig 3c, the fluorescence intensity of the HCG  
256 response to GSH gradually increased in a GSH concentration dependent manner.  
257 When the control group only was incubated with 10  $\mu$ M HCG, it was obvious that a  
258 red fluorescence was observed in HT-29 cells. This result indicated that HCG could  
259 detect endogenous GSH in living cells. When 2mM NEM was introduced in HT-29

260 cells prior to, and all other procedures were consistent with the above mentioned  
 261 conditions, only weak red fluorescence was observed the confocal microscopy image  
 262 of HT-29 cells. These results were consistent with the flow cytometry results. Similar  
 263 results were achieved with MCF-7 cells and HepG2 cells (Fig S5). Therefore,  
 264 according to these results, it has been suggested that the probe HCG can be an  
 265 effective tool for detecting GSH in living cells.



266

267 **Fig 3. Flow cytometry analysis of GSH and confocal microscopy images of GSH in HT-29**268 **cells using HCG.** a) Cells were pretreated with GSH (0, 0.2, 0.5, 1.0 mM) at 37°C for 30 min and

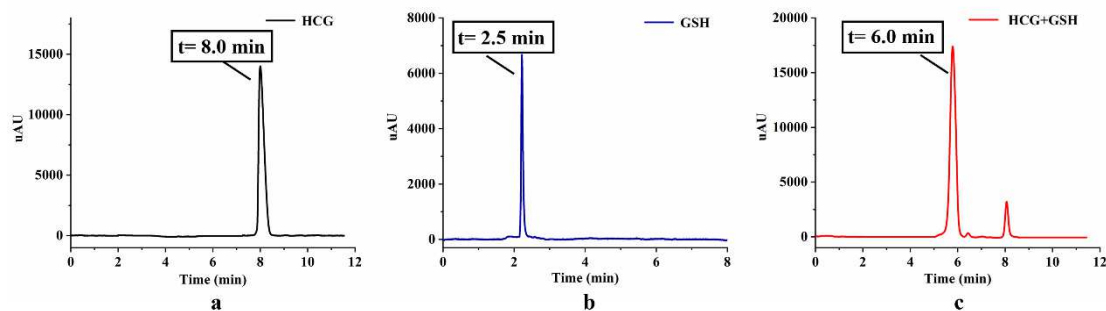
269 then stained with 10 μM HCG for 15 min before flow cytometry analysis; b) Normalized

270 fluorescence intensity of flow cytometry data; c) Cells were pretreated with varying  
271 concentrations of GSH or NEM at 37°C for 30 min, and then treated with 10 µM HCG for 15 min  
272 before obtaining the confocal microscopy images. Scale bar: 20 µm. Representative images from  
273 replicate experiments (n = 5) are shown.

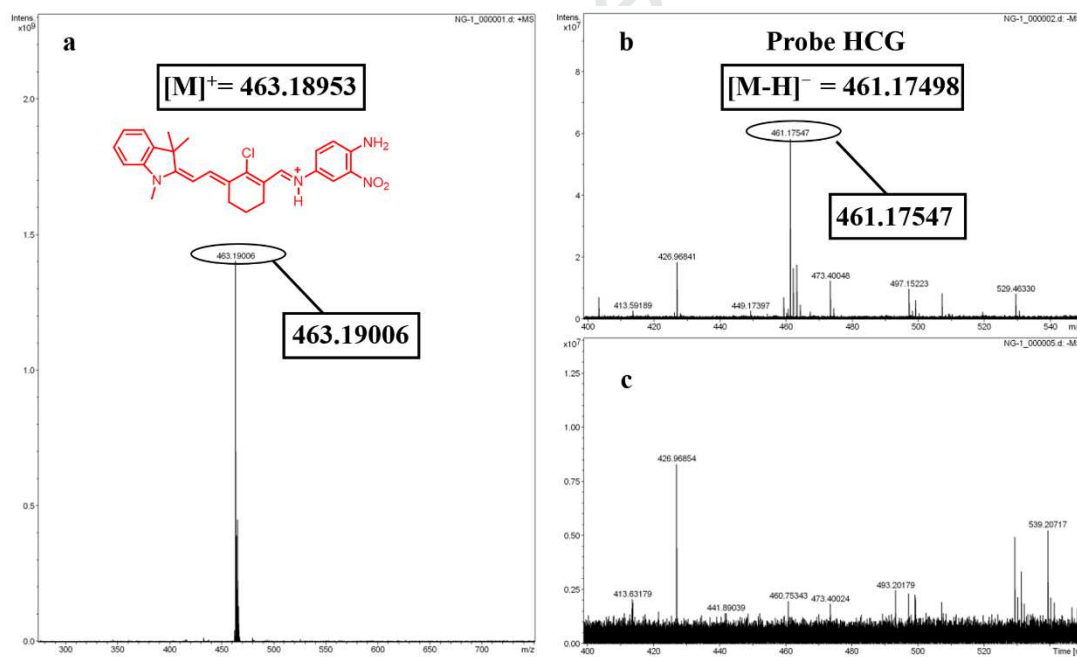
### 274 3.5 The plausible mechanism

275 To gain insights into the mechanism of the HCG fluorescent response to GSH,  
276 HCG (10 µM) was reacted with GSH (500 µM) in 5 mL of methanol. The reaction  
277 mixture was measured by high-performance liquid chromatography (HPLC). The  
278 retention time of the HCG, GSH and the reaction product were recorded. As it is  
279 shown in Fig 4, the retention time of the HCG was 8.0 min (Fig 4a), and the retention  
280 time of GSH was 2.5 min (Fig 4b). However, the reaction product has a strong signal  
281 at 6.0 min (Fig 4c). Additionally, the reaction mixture was surveyed with a  
282 high-resolution liquid chromatograph mass spectrometer (HR-LC-MS). In positive ion  
283 mode of the HRMS analysis, the thiol-imine Michael adduct was found to have a m/z  
284 of 770.27025 (Fig S6) and HCGS was found to have a m/z of 463.19006 in the mass  
285 spectra. However, in negative ion mode of the HRMS analysis, the HCGS wasn't  
286 found in mass spectra and the probe HCG could be found to have a m/z of 461.17547  
287 in the mass spectra. This indicated that HCG reacted with GSH to form a thiol-imine  
288 adduct and then the thiol-imine adduct decomposed into a protonatable Schiff base,  
289 which couldn't be measured in negative ion mode on the mass spectrometer (Fig S6  
290 and Fig 5). The plausible mechanism was speculated that firstly, the non-red  
291 fluorescent HCG reacted with GSH to gain a thiol-imine adduct [47]. Because the  
292 thiol-imine Michael addition were unstable, the thiol-imine adduct was easily

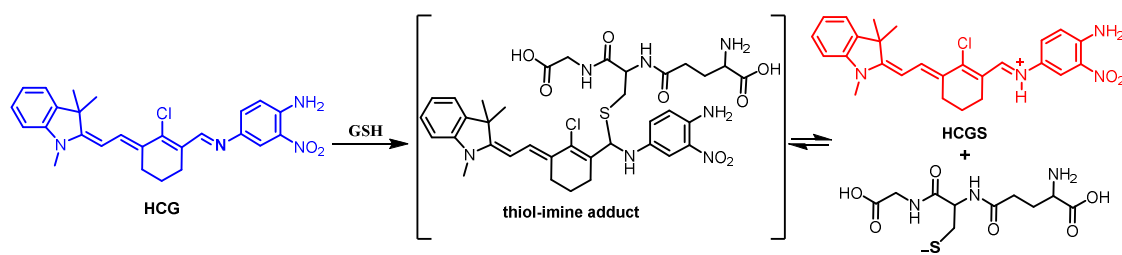
293 decomposed into a protonatable Schiff base of HCG. The protonatable Schiff base of  
 294 HCG was generated in the reaction mixture and led to a red shift in the optical signal  
 295 (Scheme 3).



296  
 297 **Fig 4. The reaction between 500  $\mu\text{M}$  GSH and 10  $\mu\text{M}$  HCG was tracked by HPLC. a) the**  
 298 **retention time of HCG; b) the retention time of the GSH; c) the retention time of the reaction**  
 299 **product.**



300  
 301 **Fig 5. High resolution mass spectrum of 10  $\mu\text{M}$  HCG reacted with 500  $\mu\text{M}$  GSH. a) the**  
 302 **positive ion mode of reaction product; b) the negative ion mode of probe HCG; c) the negative ion**  
 303 **mode of the reaction product.**



306 **Scheme 3. Proposed detection mechanism of probe HCG for GSH.**

307 3.6 The application of HCG *in vivo*

308 To investigate the application of HCG to respond to GSH *in vivo*, the BALB/c

309 mice were pretreated with GSH (1 mM) and saline for 5 min, and then injected with

310 HCG (10  $\mu$ M, 100  $\mu$ L in 1:99 DMSO/saline, v/v). After 30 min, fluorescence images

311 were obtained by a small-animal *in vivo* imaging system (IVIS). There was a

312 fluorescence signal in the control group. GSH was introduced into the mice ahead of

313 time, and the fluorescence signal was greatly improved in the liver of the mice (Fig 6),

314 indicating that the probe HCG can detect endogenous GSH by the blood circulation in

315 mice. Because GSH is gathered and metabolized first in the liver of the mice by the

316 blood circulation [48-50], the probe HCG enters the liver and detects GSH to lead to a

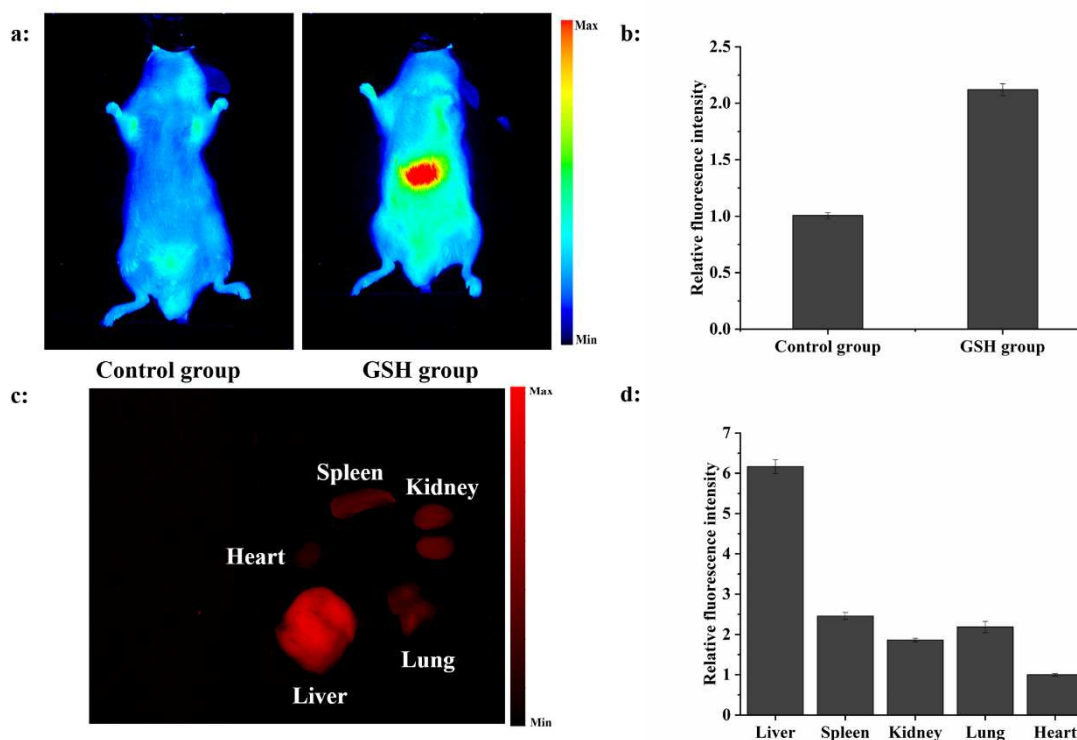
317 fluorescence signal *in vivo*. In GSH group mice, the liver had a more obvious

318 fluorescence signal than the other organs, because the liver contains abundant GSH.

319 In this regard, HCG is an effective probe to detect changes in the concentrations of

320 GSH *in vivo* and can provide a visual signal from IVIS.

321



322

323 **Fig 6. Fluorescence imaging of BALB/c mice.** a) HCG was applied to a control group and a GSH  
 324 group with IVIS; b) Relative fluorescence intensity of the control group and GSH group; c) *Ex*  
 325 *vivo* fluorescence imaging: the separated organs from the sacrificed GSH group mice; d) Relative  
 326 fluorescence intensity of the separated organs from the GSH group.

#### 327 4. Conclusions

328 In summary, the near-infrared fluorescent probe HCG was designed and  
 329 developed successfully based on the Schiff base red shift for the detection of GSH.  
 330 HCG shows high selectivity to discriminate between GSH and similar amino acids,  
 331 shows a fast response time (30 s) and has a low actual detection limit of 0.5  $\mu\text{M}$  *in*  
 332 *vitro*. Due to the low cytotoxicity and great near-infrared properties, HCG was  
 333 successfully applied to the fluorescence imaging of endogenous GSH in HT-29,  
 334 MCF-7 and HepG2 cells. Last, we studied the bio-distribution of GSH in BALB/c  
 335 mice through fluorescence imaging of HCG. With facile preparations, this strategy

336 can provide an effective tool to detect GSH levels. The results suggest that HCG has  
337 potential utility in biological science research.

### 338 **Acknowledgements**

339 We appreciate the staff from the Analysis and Testing Center of Huazhong  
340 University of Science and Technology for their technical assistance. The research was  
341 supported by grants from the National Natural Science Foundation of China (No.  
342 81373300) and Hubei Provincial Natural Science Foundation of China.

### 343 **Appendix A. Supplementary data**

344 Supplementary data related to this article can be found at <http://xxxxxxxxxxxxxxx>.

345

346

### 347 **References**

- 348 [1] Sedgwick AC, Han HH, Gardiner JE, Bull SD, He XP, James TD. The  
349 development of a novel AND logic based fluorescence probe for the detection of  
350 peroxynitrite and GSH. *Chem Sci* 2018; 9: 3672-6.
- 351 [2] Chen X, Zhou Y, Peng X, Yoon J. Fluorescent and colorimetric probes for  
352 detection of thiols. *Chem Soc Rev* 2010; 39: 2120-35.
- 353 [3] Weerapana E, Wang C, Simon GM, Richter F, Khare S, Dillon MB, Bachovchin  
354 DA, Mowen K, Baker D, Cravatt BF. Quantitative reactivity profiling predicts  
355 functional cysteines in proteomes. *Nature* 2010; 468: 790-5.
- 356 [4] Townsend DM, Tew KD, Tapiero H. The importance of glutathione in human  
357 disease. *Biomed Pharmacother* 2003; 57: 145-55.

- 358 [5] Saito C, Zwingmann C, Jaeschke H. Novel mechanisms of protection against  
359 acetaminophen hepatotoxicity in mice by glutathione and N-acetylcysteine.  
360 Hepatology 2010; 51: 246-54.
- 361 [6] Homma T, Fujii J. Application of glutathione as anti-oxidative and anti-aging  
362 drugs. Curr Drug Metab 2015; 16: 560-71.
- 363 [7] Tapiero H, Townsend DM, Tew KD. The antioxidant role of selenium and  
364 seleno-compounds. Biomed Pharmacother 2003; 57: 134-44.
- 365 [8] Enami S, Hoffmann MR, Colussi AJ. OH-radical specific addition to glutathione  
366 S-atom at the air–water interface: relevance to the redox balance of the lung  
367 epithelial lining fluid. J Phys Chem Lett 2015; 6: 3935-43.
- 368 [9] Pittet MJ, Weissleder R. Intravital imaging. Cell 2011; 147: 983-91.
- 369 [10] James ML, Gambhir SS. A molecular imaging primer: modalities, imaging agents,  
370 and applications. Physiol Rev 2012; 92: 897-965.
- 371 [11] Yin C, Huo F, Zhang J, Martínez-Máñez R, Yang Y, Lv H, Li S. Thiol-addition  
372 reactions and their applications in thiol recognition. Chem Soc Rev 2013; 42:  
373 6032-59.
- 374 [12] Niu LY, Chen YZ, Zheng HR, Wu LZ, Tung CH, Yang QZ. Design strategies of  
375 fluorescent probes for selective detection among biothiols. Chem Soc Rev 2015;  
376 44: 6143-60.
- 377 [13] Huang Y, Zhou J, Feng H, Zheng J, Ma HM, Liu W, Tang C, Ao H, Zhao M, Qian  
378 Z. A dual-channel fluorescent chemosensor for discriminative detection of  
379 glutathione based on functionalized carbon quantum dots. Biosens Bioelectron

- 380 2016; 86: 748-55.
- 381 [14]Li Y, Liu W, Zhang P, Zhang H, Wu J, Ge J, Wang P. A fluorescent probe for the  
382 efficient discrimination of Cys, Hcy and GSH based on different cascade  
383 reactions. *Biosens Bioelectron* 2017; 90: 117-24.
- 384 [15]Fu ZH, Han X, Shao Y, Fang J, Zhang ZH, Wang YW, Peng Y. Fluorescein-based  
385 chromogenic and ratiometric fluorescence probe for highly selective detection of  
386 cysteine and its application in bioimaging. *Anal Chem* 2017; 89: 1937-44.
- 387 [16]Jung HS, Chen X, Kim JS, Yoon J. Recent progress in luminescent and  
388 colorimetric chemosensors for detection of thiols. *Chem Soc Rev* 2013; 42:  
389 6019-31.
- 390 [17]Lu J, Song Y, Shi W, Li X, Ma H. A long-wavelength fluorescent probe for  
391 imaging reduced glutathione in live cells. *Sens Actuators B Chem.* 2012; 161:  
392 615-20.
- 393 [18]Lee S, Li J, Zhou X, Yin J, Yoon J. Recent progress on the development of  
394 glutathione (GSH) selective fluorescent and colorimetric probes. *Coord Chem*  
395 *Rev* 2018; 366: 29-68.
- 396 [19]Umezawa K, Yoshida M, Kamiya M, Yamasoba T, Urano Y. Rational design of  
397 reversible fluorescent probes for live-cell imaging and quantification of fast  
398 glutathione dynamics. *Nat Chem* 2017; 9: 279-86.
- 399 [20]Yi L, Li H, Sun L, Liu L, Zhang C, Xi Z. A highly sensitive fluorescence probe  
400 for fast thiol quantification assay of glutathione reductase. *Angew Chem Int Ed*  
401 2009; 121: 4094-97.

- 402 [21] Yin J, Kwon Y, Kim D, Lee D, Kim G, Hu Y, Ryu JH, Yoon J. Cyanine-based  
403 fluorescent probe for highly selective detection of glutathione in cell cultures and  
404 live mouse tissues. *J Am Chem Soc* 2014; 136: 5351-58.
- 405 [22] Chen H, Zhao Q, Wu Y, Li F, Yang H, Yi T, Huang C. Selective phosphorescence  
406 chemosensor for homocysteine based on an Iridium(III) complex. *Inorg Chem*  
407 2007; 46: 11075-81.
- 408 [23] Tang B, Xing Y, Li P, Zhang N, Yu F, Yang G. A rhodamine-based fluorescent  
409 probe containing a Se-N bond for detecting thiols and its application in living  
410 cells. *J Am Chem Soc* 2007; 129: 11666-7.
- 411 [24] Lim CS, Masanta G, Kim HJ, Han JH, Kim HM, Cho BR. Ratiometric detection  
412 of mitochondrial thiols with a two-photon fluorescent probe. *J Am Chem Soc*  
413 2011; 133: 11132-5.
- 414 [25] Ji S, Yang J, Yang Q, Liu S, Chen M, Zhao J. Tuning the intramolecular charge  
415 transfer of alkynylpyrenes: effect on photophysical properties and its application  
416 in design of OFF-ON fluorescent thiol probes. *J Org Chem* 2009; 74: 4855-65.
- 417 [26] Han B, Yuan J, Wang E. Sensitive and selective sensor for biothiols in the cell  
418 based on the recovered fluorescence of the CdTe quantum Dots-Hg(II) system.  
419 *Anal Chem* 2009; 81: 5569-73.
- 420 [27] Xia Y, Zhang H, Zhu X, Fang M, Yang M, Zhang Q, Li X, Zhou H, Yang X, Tian  
421 Y. Fluorescent probes for detecting glutathione: Bio-imaging and two reaction  
422 mechanisms. *Dyes Pigments* 2019; 163: 441-6.
- 423 [28] Lim SY, Hong KH, Kim DI, Kwon H, Kim HJ. Tunable heptamethine-azo dye

- 424 conjugate as an NIR fluorescent probe for the selective detection of mitochondrial  
425 glutathione over cysteine and homocysteine. *J Am Chem Soc* 2014; 136:  
426 7018-25.
- 427 [29]Kim Y, Mulay S, Choi M, Yu SB, Jon S, Churchill D. Exceptional time response,  
428 stability and selectivity in doubly-activated phenyl selenium-based  
429 glutathione-selective platform. *Chem Sci* 2015; 6: 5435-39.
- 430 [30]Zhang H, Liu R, Liu J, Li L, Wang P, Yao SQ, Xu Z, Sun H. A minimalist  
431 fluorescent probe for differentiating Cys, Hcy and GSH in live cells. *Chem Sci*  
432 2016; 7: 256-60.
- 433 [31]Mulay SV, Kim Y, Choi M, Lee DY, Choi J, Lee Y, Jon S, Churchill D. Enhanced  
434 doubly activated dual emission fluorescent probes for selective imaging of  
435 glutathione or cysteine in living systems. *Anal Chem* 2018; 90: 2648-54.
- 436 [32]Zhang J, Bao X, Zhou J, Peng F, Ren H, Dong X, Zhao W. A  
437 mitochondria-targeted turn-on fluorescent probe for the detection of glutathione  
438 in living cells. *Biosens Bioelectron* 2016; 85: 164-70.
- 439 [33]Gong D, Han S, Iqbal A, Qian J, Cao T, Liu W, Liu W, Qin W, Guo H. Fast and  
440 selective two-stage ratiometric fluorescent probes for imaging of glutathione in  
441 living cells. *Anal Chem* 2017; 89: 13112-9.
- 442 [34]Gong D, Ru J, Cao T, Qian J, Liu W, Iqbal A, Liu W, Qin W, Guo H. Two-stage  
443 ratiometric fluorescent responsive probe for rapid glutathione detection based on  
444 BODIPY thiol-halogen nucleophilic mono- or disubstitution. *Sens Actuators B*  
445 *Chem* 2018; 258: 72-9.

- 446 [35] Mizukami S. Targetable fluorescent sensors for advanced cell function analysis. J  
447 Photochem Photobiol C Photochem Rev 2017; 30: 24-35.
- 448 [36] Sun W, Guo S, Hu C, Fan J, Peng X. Recent Development of Chemosensors  
449 Based on Cyanine Platforms. Chem Rev 2016; 116: 7768-817.
- 450 [37] Hoischen D, Steinmuller S, Gartner W, Buss V, Martin HD. Merocyanines as  
451 Extremely Bathochromically Absorbing Chromophores in the Halobacterial  
452 Membrane Protein Bacteriorhodopsin. Angew Chem Int Ed 1997; 36: 1630-3.
- 453 [38] Yapici I, Lee KSS, Berbasova T, Nosrati M, Jia X, Vasileiou C. "Turn-on" protein  
454 fluorescence: in situ formation of cyanine dyes. J Am Chem Soc 2015; 137:  
455 1073-80.
- 456 [39] Oshikawa Y, Ojida A. PET-dependent fluorescence sensing of enzyme reactions  
457 using the large and tunable pKa shift of aliphatic amines. Chem Commun (Camb)  
458 2013; 49: 11373-5.
- 459 [40] Puyol M, Encinas C, Rivera L, Miltsov S, Alonso J. Characterisation of new  
460 norcyanine dyes and their application as pH chromoionophores in optical sensors.  
461 Dyes Pigments 2007; 73: 383-9.
- 462 [41] Zhang S, Wang Q, Liu X, Zhang J, Yang XF, Li Z, Li H. Sensitive and selective  
463 fluorescent probe for selenol in living cells designed via a pKa shift strategy. Anal  
464 Chem 2018; 90: 4119-25.
- 465 [42] Zhang J, Wang J, Liu J, Ning L, Zhu X, Yu B, Liu X, Yao X, Zhang H.  
466 Near-infrared and naked-eye fluorescence probe for direct and highly selective  
467 detection of cysteine and its application in living cells. Anal Chem 2015; 87:

- 468 4856-63.
- 469 [43]Rajasekaran K, Sarathi A, Ramalakshmi S. Micellar catalysis in the  
470 retro-Knoevenagel reaction of ethyl- $\alpha$ -cyanocinnamates. *J Chem Sci* 2008; 120:  
471 475-80.
- 472 [44]Rurack K, Spieles M, Fluorescence quantum yields of a series of red and  
473 near-infrared dyes emitting at 600-1000 nm. *Anal Chem* 2011; 83: 1232-42.
- 474 [45]Becker PS, Cohen CM, Lux SE. The effect of mild diamide oxidation on the  
475 structure and function of human erythrocyte spectrin. *J Biol Chem* 1986; 261:  
476 4620-8.
- 477 [46]Yellaturu CR, Bhanoori M, Neeli I, Rao GN. N-Ethylmaleimide inhibits  
478 platelet-derived growth factor BB-stimulated Akt phosphorylation via activation  
479 of protein phosphatase 2A. *J Biol Chem* 2002; 277: 40148-55.
- 480 [47]Stacy GW, Day RI, Morath RJ. Schiff bases and related substances. II. reactions  
481 of thiols with N-benzylideneaniline and N-benzylideneanthranilic acid. *J Am*  
482 *Chem Soc* 1955; 77: 3869-73.
- 483 [48]Liang M, Zheng X, Tu L, Ma Z, Wang Z, Yan D, Shi Z. The liver-targeting study  
484 of the N-galactosylated chitosan in vivo and in vitro, *Artif Cells Nanomed*  
485 *Biotechnol* 2014; 42: 423-8.
- 486 [49]Triger DR. The liver as an immunological organ. *Hepatology* 1976; 71: 162-4.
- 487 [50]Zhang Y, Zheng Z, Yang X, Pan X, Yin L, Huang X, Li Q, Shu Y, Zhang Q, Wang  
488 K. A sensitive and rapid radiolabelling method for the in vivo pharmacokinetic  
489 study of lentinan. *Food Funct* 2018; 9: 3114-25.

1

## Highlights

- 2 ● A turn-on near-infrared fluorescent probe was developed for monitoring  
3 reduced glutathione (GSH) by facile synthetic procedures
- 4 ● The probe can detect GSH based on the red shift of Schiff base, which had  
5 high sensitivity, high selectivity, low detection limit and fast response time *in*  
6 *vitro*.
- 7 ● The probe served as bioimaging tool for detecting endogenous and exogenous  
8 GSH in three living cells.
- 9 ● The bio-distribution of GSH in the BALB/c mice was studied through  
10 fluorescent imaging of HCG